

Solutions for downslope pipeline walking on a seabed with a peaky tri-linear soil resistance model

Adriano Castelo

PhD Candidate, The University of Western Australia
UWA (M053), 35 Stirling Highway CRAWLEY WA 6009, Australia
21445298@student.uwa.edu.au

David White

Professor, The University of Southampton
Boldrewood Innovation Campus, Southampton, SO16 7QF, UK
david.white@soton.ac.uk

Yinghui Tian

Associate Professor, The University of Melbourne
Parkville, 3010, Australia
yinghui.tian@unimelb.edu.au

ABSTRACT

Offshore pipelines used for transporting hydrocarbons are cyclically loaded by great variations of pressure and temperature. These variations can induce axial instability in such pipelines. This instability may cause the pipelines to migrate globally along their length; an effect known as pipeline walking. Traditional models of pipeline walking have considered the axial soil response as rigid-plastic (RP); however, such behaviour does not match observations from physical soil tests. It leads to inaccurate estimates of walking rate (WR) per cycle and over design. In this paper, a tri-linear (3L) soil resistance model is used to represent seabed resistance to investigate the behaviour of pipeline walking. Different parameters, i.e. shapes and properties of tri-linearity (within the peaky soil model type) have been considered leading to a closed-form solution. This solution improves understanding of the main properties involved in the peaky tri-linear soil behaviour by providing a set of analytical expressions for pipe walking, which were benchmarked and validated against a set of finite element analyses.

KEYWORDS

axial resistance; pipe-soil interaction; pipeline walking; finite-element modelling; offshore engineering

1 **1 INTRODUCTION**

2 As offshore oil and gas industry increasingly explores deep water reservoirs,
3 offshore pipelines become progressively important. Under operational load cycles, they
4 expand and contract in response to temperature and pressure changes. However, these
5 expansion and contraction cycles may have an asymmetric behaviour due to seabed
6 slopes or other factors, such as multiphasic flow (Bruton *et al.*, 2010), and thermal
7 transients (Carr *et al.*, 2006). The asymmetric expansion and contraction directly impacts
8 the stability of these pipelines causing them to migrate in one direction, which generates
9 the phenomenon known as pipeline walking (Carr *et al.*, 2003). Pipeline walking
10 increases cost and risk and may severely impact the subsea system (Tornes *et al.*, 2000).
11 It may overstress connections, alter loads and strains in any engineered lateral buckle
12 and may also present the need for anchoring. Hence, accurately identifying and
13 estimating pipeline walking is necessary to decrease the risk of production loss and
14 environmental impact, and it can significantly decrease project development costs.

15 Presently, the common practice in the industry is to evaluate pipeline walking
16 during the design phase using a set of analytical formulations as per Bruton *et al.* (2010).
17 These calculations consider various aspects, such as operational (temperature, pressure,
18 etc.), environmental (seabed overall slope angle, soil friction coefficient, etc.) and
19 physical pipeline properties (length, steel wall thickness, etc.); but still imply some
20 limitations such as the idealised rigid-plastic pipe-soil interaction, and the single seabed
21 slope. Accurately evaluating high-temperature and high-pressure pipelines for
22 downslope pipeline walking is of paramount importance to the industry because these

23 conditions are commonly found in fully operational areas, such as the Gulf of Mexico,
24 North Sea and Northwest Australia, as well as in frontier locations, which are still in early
25 stages of exploration, such as the Brazilian Pre-Salt and the Arctic Region. The analytical
26 formulation is based on an idealised soil resistance model and can provide inaccurate
27 walking rates. Then, the assessment requires further improvement of the soil resistance
28 model to overcome this limitation.

29 Costly and time demanding finite element analyses are used to confirm walking
30 behaviour and to generate a reliable walking rate. However, emerging academic
31 research (Castelo *et al.*, 2019; Castelo *et al.*, in press b) demonstrates that, if more
32 realistic soil behaviour is considered in the analytical formulae, the requirement for time
33 demanding and expensive finite element analyses can be reduced.

34 Although the formulation developed by Castelo *et al.* (2019) and Castelo *et al.* (in
35 press b) generate significant cost-savings and improve efficiency, they are limited to a
36 single soil model type, i.e. elastic-plastic (elastic-perfectly-plastic and non-linear elastic-
37 plastic, respectively). Therefore, further improvement is needed to capture the walking
38 behaviour with soils that develop a peak breakout resistance before reaching a plastic
39 plateau, as commonly seen in the operational areas mentioned above, and thus the
40 accuracy of pipeline walking results for analytical formulae is increased.

41 It has been found that there is a significant lack of knowledge about the influence
42 of pipe-soil interaction models on pipeline walking. Rong *et al.* (2009) acknowledge that
43 there is such an influence by stating: *“The axial mobilization distances may have*
44 *significant effects on the axial walking. Unfortunately, limited literature is available*

45 *about this topic.*" The latest joint industry project (JIP) research program, the SAFEBUCK
46 JIP (Bruton *et al.*, 2007; Bruton and Carr, 2011a; Bruton and Carr, 2011b) has not
47 clarified what should be the treatment for axial pipe-soil interaction, when pipeline
48 walking is assessed. The SAFEBUCK JIP solely focused on the ideal rigid-plastic pipe-soil
49 interaction model.

50 In addition, the pipe-soil interaction standard, DNVGL-RP-F114 (DNVGL, 2017)
51 mentions: "*In assessments of pipe walking, a low value of mobilisation distance creates a*
52 *higher rate of axial walking. To be conservative, a bi-linear fit to the non-linear response*
53 *should be a tangent fit to the initial part of the axial force-displacement response, which*
54 *represents the elastic recoverable part*". Hence, no guidance has yet been given on how
55 to treat non-rigid-plastic soil models on pipeline walking assessments.

56 This paper investigates the impact on pipeline walking of a tri-linear soil
57 resistance model accounting for a peak break-out behaviour. It starts by a brief literature
58 review of the present methodology used to estimate the walking rate for elastic-plastic
59 soils (Castelo *et al.*, 2019; Castelo *et al.*, in press b). It then builds on the previous
60 knowledge to generate theoretical expressions for pipeline walking on peaky tri-linear
61 soils. Next, finite element analyses are performed to provide confirmation on the
62 theoretical framework. Finally, this paper generates a solution that allows an adjustment
63 for the original rigid-plastic analytical formulation (Bruton *et al.*, 2010), so that the
64 requirement for finite element analyses can be avoided.

65 **2 BACKGROUND TO PIPELINE WALKING**

66 **2.1 Downslope mechanism**

67 The seabed slope generates an asymmetry between the start-up (SUp) and
68 shutdown (SDown) phases in the effective axial force (EAF) profile for a fully mobilised
69 pipeline, as illustrated in Figure 1, where the rigid-plastic soil condition is considered.
70 This asymmetry causes the virtual anchor sections (VAS) to be separated by a given
71 distance, X_{ab} . For rigid-plastic soil representations, the virtual anchor sections
72 correspond to the maximum absolute effective axial force along the pipeline length, L .
73 Then, the distance X_{ab} can be associated to the axial displacement, δ_x , from a particular
74 load phase (start-up and shutdown phases), as presented by Figure 2. Because it tends to
75 create unbalanced displacements during different loading stages, the asymmetry in the
76 effective axial force profile is presently understood to be root cause of pipeline walking.

77 Accounting for more realistic soil conditions, the distance X_{ab} cannot be
78 associated with maximum effective axial force. Therefore, X_{ab} must be associated with
79 the stationary points (SP), as thoroughly explained in Castelo *et al.* (2019).

80 **2.2 Pipe-soil response**

81 Previous research on pipeline walking has treated soils as rigid-plastic (Carr *et al.*,
82 2003; Carr *et al.*, 2006; Bruton *et al.*, 2010) or as elastic-plastic (Castelo *et al.*, 2019;
83 Castelo *et al.*, in press b). However, it is known that some soils behave much more
84 complex, usually producing first a breakout peak resistance and then decreasing their
85 resistance to a residual plastic level.

86 Although many other studies, such as White *et al.* (2011), have already
87 investigated peaky soils in general terms, none has gone through the specific impact on
88 pipeline walking. This paper focuses on a soil representation that accounts for breakout
89 soil resistance using a peaky tri-linear (3L) soil representation and how pipeline walking
90 may change due to this different soil condition.

91 **3 PROBLEM DEFINITION**

92 Downslope pipeline walking is dependent on three types of properties:
93 environmental, operational and those of the pipeline. This paper's parametric study uses
94 typical parameter ranges for these three properties.

95 The environmental parameters include seabed slope angle, β , and residual
96 friction coefficient, μ , taken to be 2 ° and 0.25, respectively. The operational parameters
97 include temperature variation, ΔT , and pipe submerged weight, W , assumed to be 100 °C
98 and 0.4 kN/m, respectively. The physical pipeline properties include steel outside
99 diameter, OD , steel wall thickness, t , and length, taken to be 0.3239 m, 0.0206 m and
100 5000 m, respectively. Some additional environmental properties were taken as variables
101 for the parametric study, and they are related to the pipe-soil response (cases i - iv). The
102 full list of properties and parameters used in this study are provided in Table 1 and Table
103 2.

104 Figure 3 presents a schematic axial force-displacement response for an ideal set
105 of peaky tri-linear soil cases. As investigated in White *et al.* (2011), it is known that
106 various aspects affect the cyclic behaviour of peaky soils. These aspects may be related,
107 but not limited, to the time interval between distinct movements, the varying pipeline

108 embedment, etc. As a result, this paper takes into account two different extreme
109 conditions for the cyclic load phases:

- 110 • “EqualPeaks”;
- 111 • “NoSUpPeak”.

112 As the conditions’ names suggest, the first condition, “EqualPeaks”, behaves with
113 equal peaks for both loading and unloading phases – start-up and shutdown.
114 Alternatively, the second condition, “NoSUpPeak”, behaves with no peak for start-up
115 phases, while peaky for shutdown phases. There is no clear understanding in the
116 literature of why the peak may exist for one load phase, while it may not occur for
117 another load phase, but this may be due to the differing waiting periods causing
118 different levels of consolidation or thixotropy (White et al. 2011). For example,
119 shutdowns are generally shorter duration than operating periods.

120 Consequently, the axial force-displacement responses, shown in Figure 3, need to
121 be updated to account for cyclic movements. Figure 4 shows the update to Figure 3,
122 presenting three hypothetical load phases for “EqualPeaks” and “NoSUpPeak”
123 conditions. The small numbered arrows indicate the loading path for each of the
124 conditions (“EqualPeaks” on top, and “NoSUpPeak” at the bottom of Figure 4).

125 According to previous experience (Castelo *et al.*, 2019; Castelo *et al.*, in press b),
126 the first load phase is not representative for the cyclic walking behaviour. At the initial
127 state, the nodes will displace a shorter distance to reach the relevant (either peak or
128 residual) force levels. Therefore, for simplicity, it is assumed that the first load phase

129 does not peak; while for the cyclic load phases it will peak as prescribed by the
130 “EqualPeaks” or “NoSUpPeak” conditions.

131 In addition, although the authors acknowledge that intermediate peak cases may
132 occur in between “EqualPeaks” and “NoSUpPeak” conditions, these intermediate
133 conditions would be enveloped by these two extreme conditions. For this reason, the
134 intermediate cases are disregarded in this paper.

135 **4 ELASTIC-PERFECTLY-PLASTIC SOLUTION FOR PIPELINE WALKING**

136 From Castelo *et al.* (in press b) it is known that the walking rate for an elastic-
137 plastic pipe-soil response, WR_{EP} , can be obtained simply by subtracting twice the
138 equivalent mobilisation displacement, δ_{mobEQ} , from the walking rate for rigid-plastic soil,
139 WR_{RP} , as shown by equation (1):

$$WR_{EP} = WR_{RP} - 2 * \delta_{mobEQ} \quad (1)$$

140 where the walking rate for rigid-plastic soil can be estimated from Carr *et al.* (2006) and
141 the equivalent mobilisation displacement for a non-linear elastic-plastic pipe-soil
142 response can be obtained from Castelo *et al.* (in press b).

143 As another option, reorganizing equation (1), as also explained by Castelo *et al.*
144 (in press b), the walking rate for an elastic-plastic pipe-soil response, can be established
145 by multiplying the walking rate for rigid-plastic soil by a reduction factor based on the
146 equivalent mobilisation displacement and the non-walking mobilisation displacement,
147 δ_{null} , as presented by equation (2):

$$WR_{EP} = WR_{RP} * \left(1 - \frac{\delta_{mobEQ}}{\delta_{null}}\right) \quad (2)$$

148 where the non-walking mobilisation displacement, δ_{null} , can be achieved using equation
 149 (3) – (Castelo *et al.*, 2019):

$$\delta_{null} = \frac{WR_{RP}}{2} \quad (3)$$

150 As confirmed by Castelo *et al.* (in press b), the same reduction factor can be
 151 applied to the distance between stationary points for an elastic-plastic pipe-soil
 152 response, $X_{ab,EP}$, as presented below by equation (4):

$$X_{ab,EP} = X_{ab,RP} * \left(1 - \frac{\delta_{mobEQ}}{\delta_{null}}\right) \quad (4)$$

153 where the distance between stationary points for rigid-plastic soil, $X_{ab,RP}$, can be
 154 estimated from Bruton *et al.* (2010).

155 A parametric study has been performed using finite element analyses, to
 156 investigate the peaky tri-linear pipe-soil responses seen in Figure 4, aiming on building
 157 on equation (1) to create an accurate, simple and fast methodology to estimate pipeline
 158 walking for this pipe-soil response type.

159 5 FINITE ELEMENT METHODOLOGY

160 The finite element model used in this paper is based on a straight pipeline laid on
 161 a uniformly sloping seabed. The properties of this model are presented in Table 1 and
 162 Table 2 (soil case ii). Table 2 also presents data used for the parametric study developed
 163 later in this paper.

164 The 5000 m pipeline was represented by 5001 nodes connected by 5000 equal
 165 Euler Bernoulli beam elements (B33 – 3 dimensional 3 noded elements in Abaqus –
 166 DASSAULT SYSTÈMES, 2014), creating a 1 metre “mesh” size. An overall sketch of the
 167 finite element model used is presented by Figure 5.

168 To represent the peaky tri-linear pipe-soil interaction, the soil was modelled as a
169 set of macro elements connected to each pipeline node, which were described as user
170 elements in user subroutine UEL coded in FORTRAN computer language.

171 **5.1 Peaky tri-linear pipe-soil interaction models**

172 Two different soil conditions were modelled for this paper: the “EqualPeaks” and
173 “NoSupPeak” extreme conditions as shown in Figure 4.

174 For the “EqualPeaks” condition, the user element interface followed a constant
175 (positive) stiffness until a predefined peak elastic force, F_P , was attained. At this peak
176 force a constant (negative) stiffness was followed, so that the reaction force reduced up
177 to a residual plateau (residual plastic force, F_R). If the displacement was reversed, the
178 same behaviour could be observed for the spring-slider in the opposite direction.

179 For the “NoSupPeak” condition, the user element interface applied the same
180 forces during loading as applied in the “EqualPeaks” condition. However, for start-up
181 phases, the forces did not present the peak, because once the reaction force achieved
182 the residual plateau, no further reaction was provided and the followed stiffness at this
183 point was zero, where the forces remained in the residual plateau.

184 **5.2 Loads**

185 In the analysis, the pipeline was heated up uniformly with temperature
186 increasing to 100 °C. This value represents a combined equivalent effect of temperature
187 and pipe internal pressure (Hobbs, 1984).

188 The self-weight of the pipeline, W , and seabed slope angle, β , generate a sliding
189 component, W_{comp} , to the weight:

$$W_{comp} = W \sin \beta \quad (5)$$

190 Operational cycling was modelled by alternating the pipeline temperature
191 between the steady operational profile (start-up) and the rest condition (shutdown).

192 **5.3 Analysis description**

193 The geometry of the model was defined by a set of nodes created in a straight
194 line as previously mentioned (Section 5 and illustrated by Figure 5). Then, the analyses
195 were performed by running a sequence of load phases as follows:

- 196 1. Applying boundary conditions and UEL properties;
- 197 2. Applying gravity to pipeline;
- 198 3. Applying temperature heating-up (start-up temperature);
- 199 4. Applying temperature cooling-down (shutdown temperature);
- 200 5. Iterating phases 3 and 4 (9 times);
- 201 6. Extracting results from simulations' outputs.

202 **6 FINITE ELEMENT ANALYSIS RESULTS AND COMPARISON WITH RIGID-PLASTIC** 203 **SOLUTION**

204 Figure 6 and Figure 7 show the effective axial force and the axial displacement
205 distribution, respectively, for the "EqualPeaks" condition applied to ideal case ii.

206 Figure 8 and Figure 9 show the effective axial force and the axial displacement
207 distribution for "NoSupPeak" condition applied to ideal case ii.

208 Although, these two finite element analyses ("EqualPeaks" and "NoSupPeak")
209 provided similar results when compared to each other, as shown in Table 3, when

210 compared to the analytical calculations from Bruton *et al.* (2010), as shown in Table 4,
211 the deviation presented a remarkable margin.

212 The deviation between rigid-plastic calculations and finite element results (61 m
213 for the distance between stationary points and 0.066m/cycle for the walking rate) is
214 justified by the fact that the finite element analyses considered a more realistic soil.
215 Instead of using a basic soil approximation, rigid-plastic, the analyses considered a more
216 realistic soil response, peaky tri-linear pipe-soil interaction.

217 To estimate the realistic results for the distance between stationary points and
218 for the walking rate, a closed-form solution is outlined for the peaky tri-linear pipe-soil
219 response, as was done in Castelo *et al.* (2019) and Castelo *et al.* (in press b).

220 **7 REVISED CLOSED-FORM SOLUTION FOR THE DISTANCE BETWEEN STATIONARY**
221 **POINTS FOR PEAKY TRI-LINEAR SOILS – $X_{ab,3L}$**

222 From Castelo *et al.* (in press b) where the soil is treated as a non-linear elastic-
223 plastic spring, it is known that the distance between stationary points, $X_{ab,EP}$, is equal to
224 the distance between stationary points for rigid-plastic soils, $X_{ab,RP}$, multiplied by a
225 reduction factor, which is based on the equivalent mobilisation displacement, δ_{mobEQ} ,
226 and the non-walking mobilisation displacement, δ_{null} , as shown by equation (4).

227 Alternatively, for a peaky tri-linear pipe-soil behaviour, the equivalent
228 mobilisation displacement, δ_{mobEQ} , might be substituted by an ideal mobilisation
229 displacement, δ_{mob}' .

$$X_{ab,3L} = X_{ab,RP} * \left(1 - \frac{\delta_{mob}'}{\delta_{null}} \right) \quad (6)$$

230 **8 REVISED ANALYTICAL SOLUTION FOR THE WALKING RATE FOR PEAKY TRI-LINEAR**
 231 **SOILS – WR_{3L}**

232 From Castelo *et al.* (in press b), which treated the soil as a non-linear elastic-
 233 plastic spring, it is known that the walking rate, WR_{3L} , is equal to the walking rate for
 234 rigid-plastic soils, WR_{RP} , multiplied by a reduction factor based on the equivalent
 235 mobilisation displacement, δ_{mobEQ} , and the non-walking mobilisation displacement, δ_{null} ,
 236 as previously shown by equation (2).

237 Analogously to $X_{ab,3L}$, for a peaky tri-linear pipe-soil behaviour, the equivalent
 238 mobilisation displacement, δ_{mobEQ} , might be substituted by an ideal mobilisation
 239 displacement, δ_{mob}' .

$$WR_{3L} = WR_{RP} * \left(1 - \frac{\delta_{mob}'}{\delta_{null}}\right) \quad (7)$$

240 **9 IDEAL MOBILISATION DISTANCE – δ_{mob}'**

241 As firstly developed by Castelo *et al.* (2019) and further expanded by Castelo *et*
 242 *al.* (in press b) for the elastic correction, the tri-linear correction, $Corr_{3L}$, for the walking
 243 rate predictions can be obtained by doubling the division of the unload-reload area,
 244 $A_{Unload-Reload}$, by the variation of residual plastic force, ΔF_R . However, differently to elastic-
 245 plastic soils, peaky tri-linear pipe-soil interactions have an additional area, created by the
 246 peak resistance, but the influence of the peak resistance is so small, that this additional
 247 area can be safely ignored resulting in:

$$Corr_{3L} = 2 \left(\frac{A_{Unload-Reload}}{\Delta F_R} \right) \quad (8)$$

248 Then, following the same principles, the ideal mobilisation displacement, δ_{mob}' ,
 249 can be described with a similar procedure from Castelo *et al.* (2019) and Castelo *et al.* (in
 250 press b), as outlined by equation (9):

$$\delta_{mob}' = \frac{Corr_{3L}}{2} = \left(\frac{A_{Unload-Reload}}{\Delta F_R} \right) \quad (9)$$

251 As another option, since the soil behaves linearly, δ_{mob}' can also be written as:

$$\delta_{mob}' = \frac{F_R * \delta_{mobP}}{F_P} \quad (10)$$

252 where F_R is the residual plastic force, F_P is the peak elastic force, and δ_{mobP} is the
 253 mobilisation displacement where the peak elastic force is achieved.

254 Now, using the values provided in Table 2, δ_{mob}' was calculated for cases i - iv to
 255 be 0.065, 0.032, 0.043 and 0.052 m, respectively; while, equations (6) and (7) were
 256 rewritten, accounting for equation (10), as:

$$X_{ab,3L} = X_{ab,RP} \left(1 - \frac{F_R \delta_{mobP}}{F_P \delta_{null}} \right) \quad (11)$$

$$WR_{3L} = WR_{RP} * \left(1 - \frac{F_R \delta_{mobP}}{F_P \delta_{null}} \right) \quad (12)$$

257 Hence, using equations (11) and (12) in association to the values provided by
 258 Table 1, Table 2 and Table 4, the distance between stationary points and the walking
 259 rate were obtained, as presented by Table 5*.

260 **10 FINITE ELEMENT ANALYSES PARAMETRIC STUDY FOR PEAKY TRI-LINEAR PIPE-SOIL** 261 **INTERACTION**

262 The following parametric study validates the above solutions for the distance
 263 between stationary points' and walking rate for peaky tri-linear soils.

* The authors understand that 1 m lies inside the acceptable deviation given that this is the mesh spacing.

264 The parametric study uses the values provided in Table 1 and Table 2 as
265 previously explained in section 3. For simplicity, pipeline length, pipeline submerged
266 operational weight (accounting for content), residual friction coefficient and the overall
267 route slope were kept constant, although the soil resistance was varied, as shown, for
268 the ideal cases i - iv, in Table 2, Figure 3 and Figure 4.

269 **10.1 Ideal mobilisation displacement – δ_{mob}'**

270 Each of the parametric study cases tested had their own ideal mobilisation
271 displacement, δ_{mob}' , value according to equation (10) as shown in section 9.

272 Figure 10 presents the tri-linear correction results from the numerical solutions
273 (finite element models) plotted against the values calculated using equation (8). The
274 “EqualPeaks” and the “NoSUUpPeak” soil conditions are represented by square and
275 circular markers, respectively. The triangles represent elastic-perfectly-plastic conditions,
276 accounting for the ideal mobilisation displacement – these were used to prove the
277 applicability of the ideal mobilisation displacement methodology. Cases i, ii, iii and iv are
278 indicated in the figure.

279 Figure 10 shows a very strong agreement between the tri-linear correction
280 obtained from the finite element analysis and the results calculated using the proposed
281 equation.

282 For elastic-plastic soil conditions, when the equivalent mobilisation displacement,
283 δ_{mobEQ} , nears the value of the non-walking mobilisation displacement, δ_{null} , the walking
284 rate tends to diminish up to zero and the walking phenomenon ceases (Castelo *et al.*,
285 2019; Castelo *et al.*, in press b). Analogously, to peaky tri-linear soils, when the ideal

286 mobilisation displacement, δ_{mob}' , nears δ_{null} the walking rate also tends to diminish up to
287 zero and the walking phenomenon ceases.

288 **10.2 Distance between stationary points for peaky tri-linear soil – $X_{ab,3L}$**

289 Equation (10) is applicable to finding the ideal mobilisation displacement.
290 Consequently, equation (11) must be applicable to finding the distance between the
291 stationary points. To confirm, the finite element model outputs were compared with the
292 calculated values from equation (11).

293 Figure 11 presents the results for the distance between stationary points using
294 numerical solutions (finite element models) plotted against the values calculated using
295 equation (11). The “EqualPeaks” and the “NoSupPeak” soil conditions are represented
296 by square and circular markers, respectively. The triangles represent elastic-perfectly-
297 plastic conditions, accounting for the ideal mobilisation displacement. Cases i, ii, iii and iv
298 are indicated in the figure.

299 Figure 11 shows a very strong agreement for the distance between stationary
300 points obtained from the finite element analysis and the results calculated using the
301 proposed equation.

302 **10.3 Walking rate for peaky tri-linear soil – WR_{3L}**

303 Figure 12 presents the walking rate results from the numerical solutions (finite
304 element models) plotted against the values calculated using equation (12). The
305 “EqualPeaks” and the “NoSupPeak” soil conditions are represented by square and
306 circular markers, respectively. The triangles represent elastic-perfectly-plastic conditions,

307 accounting for the ideal mobilisation displacement. Cases i, ii, iii and iv are indicated in
308 the figure.

309 Figure 12 shows a very strong agreement between the walking rates obtained
310 from the finite element analysis and the results calculated using the proposed equation.

311 Overall, the results show that equation (12) – as presented by Table 6 – gives a
312 true representation of the effects of peaky tri-linear soil springs on pipeline walking.

313 Finally, equation (1) can be translated for peaky tri-linear soils as equation (13):

$$WR_{3L} = WR_{RP} - 2\delta_{mob}' \quad (13)$$

314 where the walking rate for peaky tri-linear soils, WR_{3L} , may be directly obtained
315 by subtracting twice the ideal mobilisation displacement, δ_{mob}' , from the walking rate for
316 rigid-plastic soils, WR_{RP} .

317 **11 OBSERVATIONS ABOUT THE EFFECTIVE AXIAL FORCE VARIATION OVER THE** 318 **DISTANCE BETWEEN STATIONARY POINTS FOR PEAKY TRI-LINEAR SOILS – $\Delta S_{S,3L}$**

319 For Castelo *et al.* (2019) and Castelo *et al.* (in press b), the effective axial force
320 variation over the distance between stationary points, ΔS_S , solution was mathematically
321 revised by making adjustments for the effective axial force physical boundaries, the axial
322 displacement, δ_x , boundary conditions and the effective axial force boundary conditions.
323 These factors directly impact the differential equation used to obtain the effective axial
324 force values and ultimately change the ΔS_S expression.

325 While obtaining the effective axial force variation over the distance between
326 stationary points is important, previous experience (Castelo *et al.*, 2019; Castelo *et al.*, in
327 press b), shows that ΔS_S revision will not have a significant impact on finding the walking
328 rate for peaky tri-linear soils. Furthermore, confidence in the numerical solutions

329 obtained in previous research, and the use of similar approaches (Castelo *et al.*, 2019;
330 Castelo *et al.*, in press b), suggest that the numerical results will be sufficient to prove
331 the applicability of equations (10), (11), (12) and (13).

332 **12 LIMITATIONS & FUTURE WORK**

333 The emerging methodology has not been tested for implications on lateral
334 buckling (also referred to as Euler buckling). It has been tested in previous stages of
335 research for various pipeline lengths, which has been proved to have no influence over
336 the overall findings (Castelo *et al.*, 2019; Castelo *et al.*, in press b). For variable slopes,
337 the authors foresee further research to be published in the near future (Castelo *et al.*, in
338 press a).

339 In general terms, there are no limitations for the applicability of this
340 methodology as long as the pipeline route respect a uniformly sloped seabed with no
341 lateral buckles.

342 **13 CONCLUSIONS & FINAL REMARK**

343 This paper provides a strategy to solve downslope pipeline walking problems
344 considering peaky tri-linear soils. Different properties of tri-linearity (within the peaky
345 soil model type) have been considered, leading to an innovative analytical solution.

346 The innovation is summarised as the multiplying factor introduced in equation
347 (12) and highlighted below:

$$\left(1 - \frac{F_R}{F_P} \frac{\delta_{mobP}}{\delta_{null}}\right) \quad (14)$$

348

349 This multiplying factor accounts for the pipe-soil interaction model properties to
350 adjust the original rigid-plastic solution in a way to make the walking assessment results
351 more accurate.

352 The new solution , based on the factor highlighted in equation (14), was
353 benchmarked and validated against a set of finite element analyses.

354 Currently applied analytical solutions do not consider the soil model type with a
355 peak, and it is known that they can provide inaccurate walking patterns.

356 Therefore, this paper resolves how the fundamental closed-form solution for
357 rigid-plastic soils must be adjusted to allow for peaky tri-linear soils reducing the
358 requirement for numerical modelling which can be time- and resource-consuming in
359 early stages of design activities, such as preliminary estimates for downslope pipeline
360 walking.

361

362 **14 ACKNOWLEDGMENT**

363 This research forms part of the activities of the Centre for Offshore Foundation
364 Systems (COFS). The authors acknowledge support from The University of Western
365 Australia, Shell, and the Australian Research Council.

366

367 **NOMENCLATURE**

3L	Tri-Linear
E	Steel Young's Modulus
EAF	effective axial force
F _P	peak elastic force
F _R	residual plastic force
JIP	joint industry project
L	pipeline length
OD	steel outside diameter
RP	rigid-plastic
SDown	shutdown phase
SUp	start-up phase
SP	stationary point
t	steel wall thickness
VAS	virtual anchor section
W	pipeline submerged weight
W _{comp}	pipeline weight component
WR	walking rate
x	axial coordinate along pipe length

X_{ab}	distance between stationary points
α	steel thermal expansion coefficient
β	seabed slope angle
ΔS_S	effective axial force variation over the distance between stationary points
ΔT	temperature variation
$\delta_{mob'}$	ideal mobilisation distance
δ_{mobP}	peak elastic force mobilisation displacement
δ_{mobR}	residual plastic force mobilisation displacement
δ_{null}	non-walking mobilisation distance
δ_x	axial displacement
μ	residual friction coefficient
ν	steel Poisson coefficient

369 REFERENCES

370

371 Bruton, D. and Carr, M. (2011a) 'Lateral Buckling and Pipeline Walking - Overview of the
372 SAFEBUCK JIP', *Proceedings of the Subsea Australasia Conference 2011*.

373 Bruton, D. and Carr, M. (2011b) 'Overview of the SAFEBUCK JIP', *Proceedings of the
374 Offshore Pipeline Technology Conference*. doi: 10.4043/21671-MS.

375 Bruton, D., Carr, M. and White, D. (2007) 'The Influence of Pipe-Soil Interaction on
376 Lateral Buckling and Walking of Pipelines - the SAFEBUCK JIP', *Proceedings of the
377 International Conference on Offshore Site Investigation and Geotechnics*.

378 Bruton, D., Sinclair, F. and Carr, M. (2010) 'Lessons Learned from Observing Walking of
379 Pipelines with Lateral Buckles, Including New Driving Mechanisms and Updated Analysis
380 Models', *Proceedings of the Offshore Technology Conference*. doi: 10.4043/20750-MS.

381 Carr, M., Bruton, D. and Leslie, D. (2003) 'Lateral Buckling and Pipeline Walking, a
382 Challenge for Hot Pipelines', *Proceedings of the Offshore Pipeline Technology
383 Conference*.

384 Carr, M., Sinclair, F. and Bruton, D. (2006) 'Pipeline Walking - Understanding the Field
385 Layout Challenges and Analytical Solutions Developed for the Safebuck JIP', *Proceedings
386 of the Offshore Technology Conference*. doi: 10.2118/120022-PA.

387 Castelo, A., White, D. and Tian, Y. (2019) 'Simple Solutions for Downslope Pipeline
388 Walking on Elastic-Perfectly-Plastic Soils', *Ocean Engineering*. Elsevier Ltd, 172, pp. 671–
389 683. doi: 10.1016/j.oceaneng.2018.11.037.

390 Castelo, A., White, D. and Tian, Y. (in press a) 'Gravity Driven Pipeline Walking on
391 Variable Slopes', *International Journal of Offshore and Polar Engineering*.

392 Castelo, A., White, D. and Tian, Y. (in press b) 'Solving Downslope Pipeline Walking on
393 Non-Linear Elastic-Plastic Soils', *Marine Structures*.

394 DASSAULT SYSTÈMES (2014) 'Abaqus 6.14 Analysis User's Manual'. Providence, RI, USA:
395 Dassault Systèmes Simulia Corporation.

396 DNVGL (2017) *DNVGL-RP-F114: Pipe-Soil Interaction for Submarine Pipelines*.

397 Hobbs, R. (1984) 'In-Service Buckling of Heated Pipelines', *Journal of Transportation
398 Engineering*, 110(2), pp. 175–189. doi: 10.1061/(ASCE)0733-947X(1984)110:2(175).

399 Rong, H., Inglis, R., Bell, G., Huang, Z., and Chan, R. (2009) 'Evaluation and Mitigation of
400 Axial Walking with a Focus on Deep Water Flowlines', *Proceedings of the Offshore
401 Technology Conference*. doi:10.4043/19862-MS

402 Tornes, K., Ose, B., Jury, J., Thomson, P. et al. (2000) 'Axial Creeping of High Temperature
403 Flowlines Caused by Soil Ratcheting', *Proceedings of the ETCE/ OMAE Joint Conference,
404 Energy for the New Millennium*. Vol. 2, pp. 1229-1240.

405 White, D., Ganesan, S., Bolton, M., Bruton, D., Ballard, J-C., Langford, T. et al. (2011)
406 'SAFEBUCK JIP - Observations of Axial Pipe-Soil Interaction from Testing on Soft Natural
407 Clays', *Proceedings of the Offshore Technology Conference*. doi: 10.4043/21249-MS.

408

409

Figure Captions List

- Figure 1 Effective axial force diagrams for start-up and shutdown phases
- Figure 2 Axial displacement diagrams for start-up and shutdown phases
- Figure 3 Tri-linear soil responses
- Figure 4 Tri-linear soil responses for cyclic movements
- Figure 5** **Effective axial force for tri-linear strategy case ii – EqualPeaks (Zoom)**
Finite element model sketch



- Figure 6
- Figure 7 Axial displacement for tri-linear strategy case ii – EqualPeaks (Zoom)
- Figure 8 Effective axial force for tri-linear strategy case ii – NoSUpPeak (Zoom)

Figure 9 Axial displacement for tri-linear strategy case ii– NoSUpPeak (Zoom)

Figure 10 Tri-linear correction results

Figure 11 Distance between stationary points results

Figure 12 Walking rate results

411

412

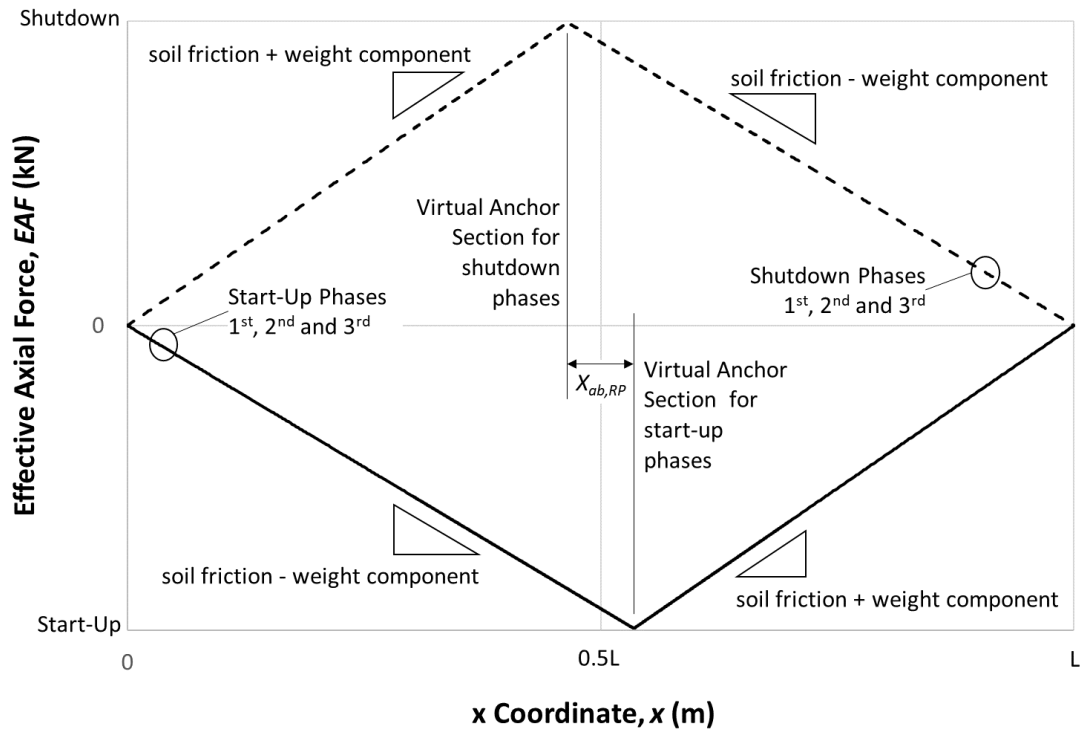
Table Caption List

Table 1	General properties
Table 2	Case properties
Table 3	Tri-linear finite element analysis results for soil case ii
Table 4	Rigid-plastic calculation results
Table 5	Analytical results
Table 6	Tri-linear finite element analyses results

413

414 FIGURES

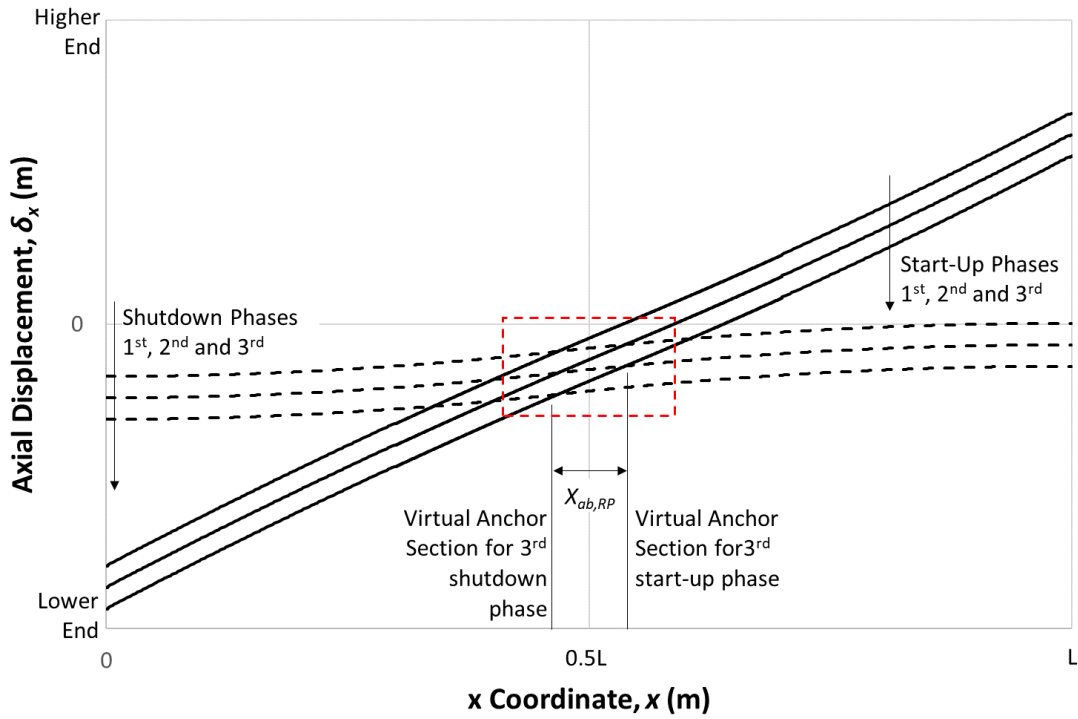
415 Figure 1 Effective axial force diagrams for start-up and shutdown phases



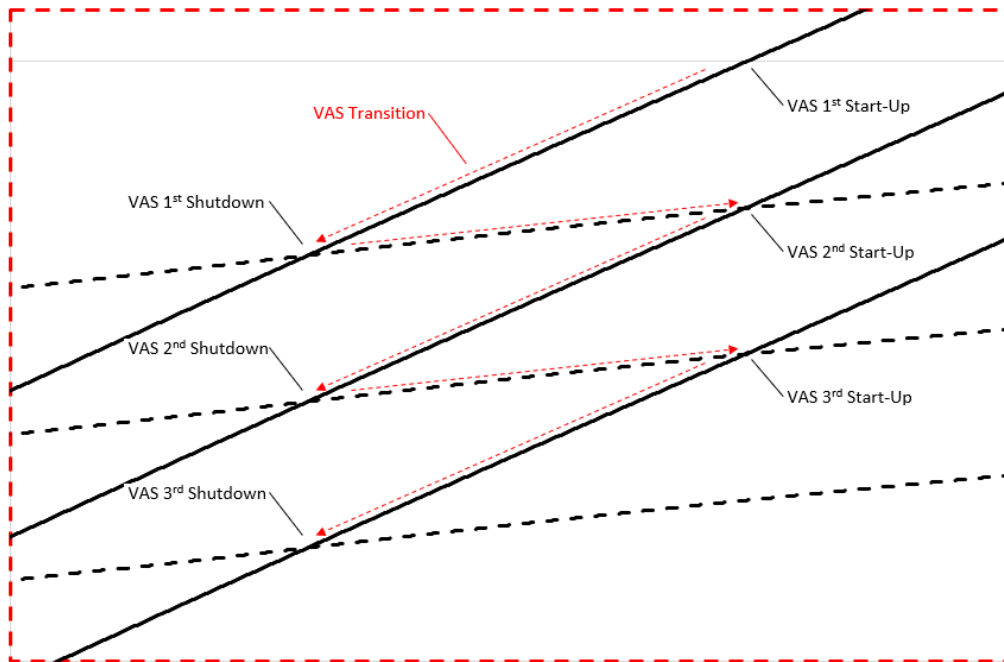
416
417

418

419 **Figure 2 Axial displacement diagrams for start-up and shutdown phases**



420

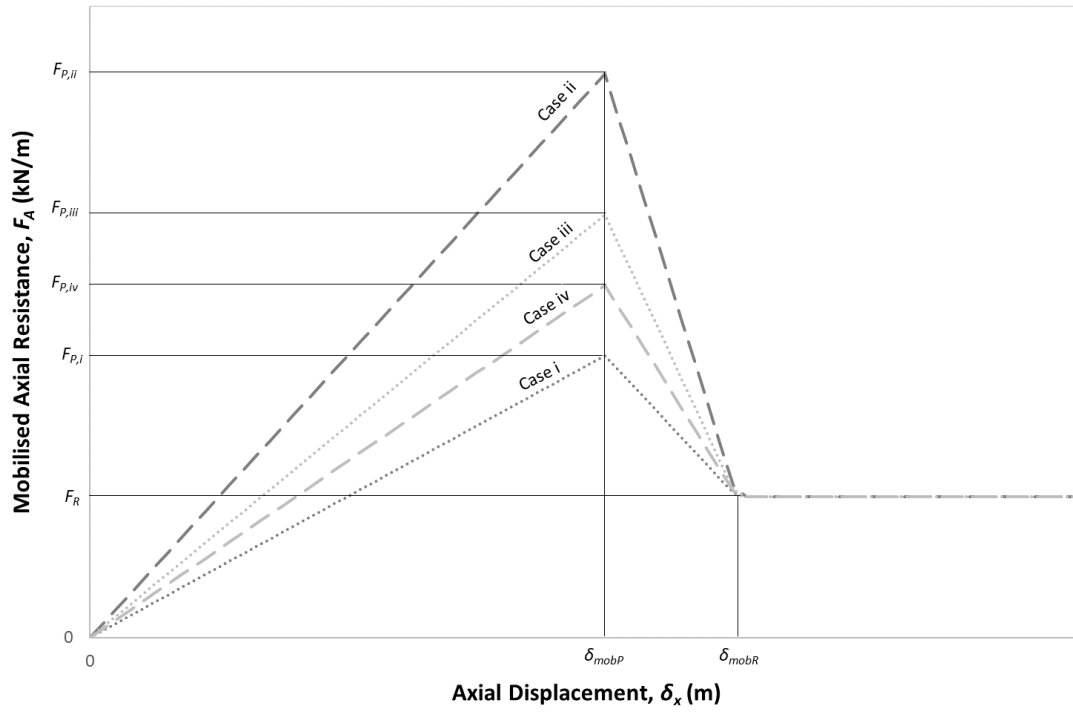


421

422

423

424 **Figure 3 Tri-linear soil responses**

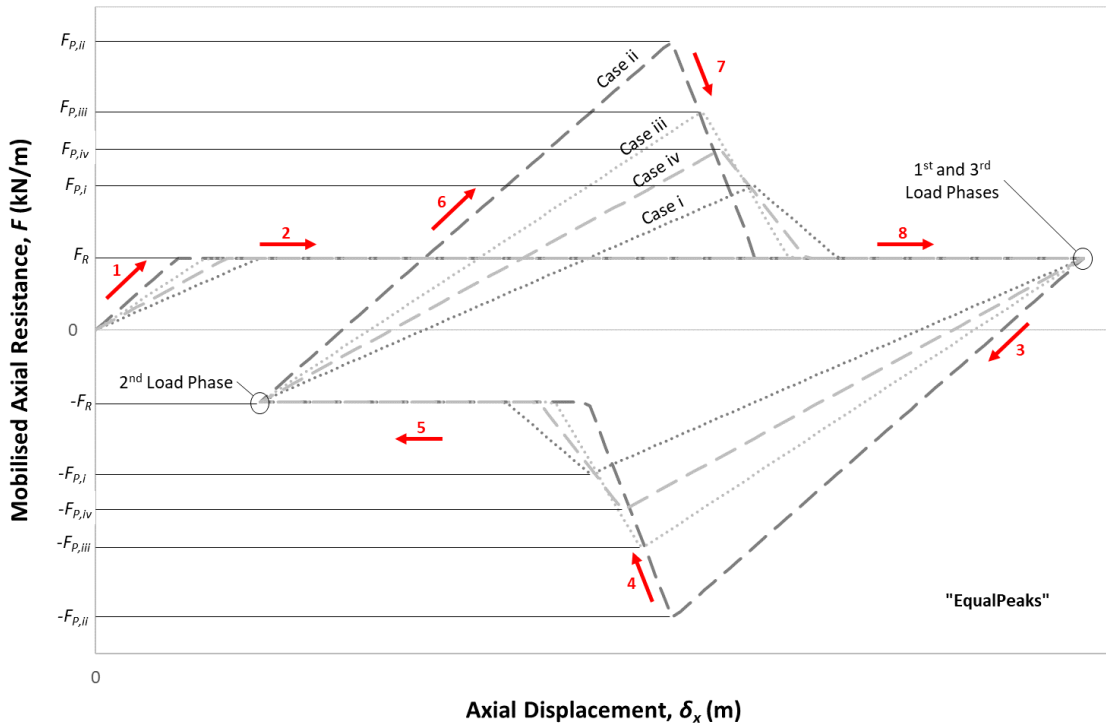


425

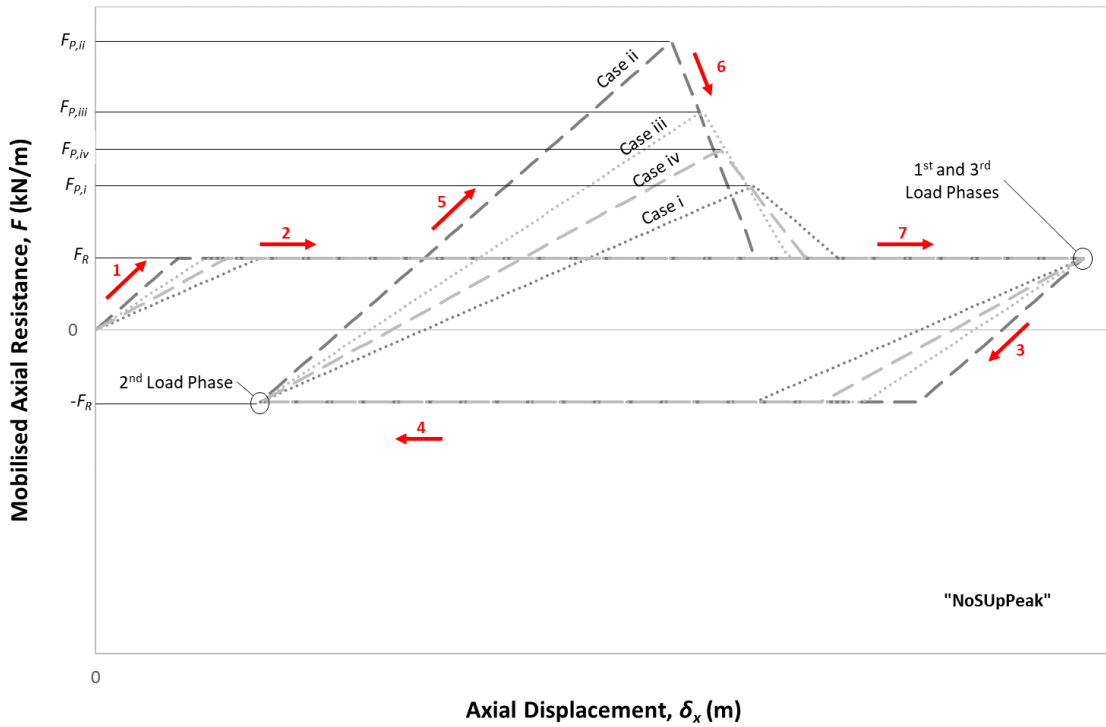
426

427

428 **Figure 4 Tri-linear soil responses for cyclic movements**



429

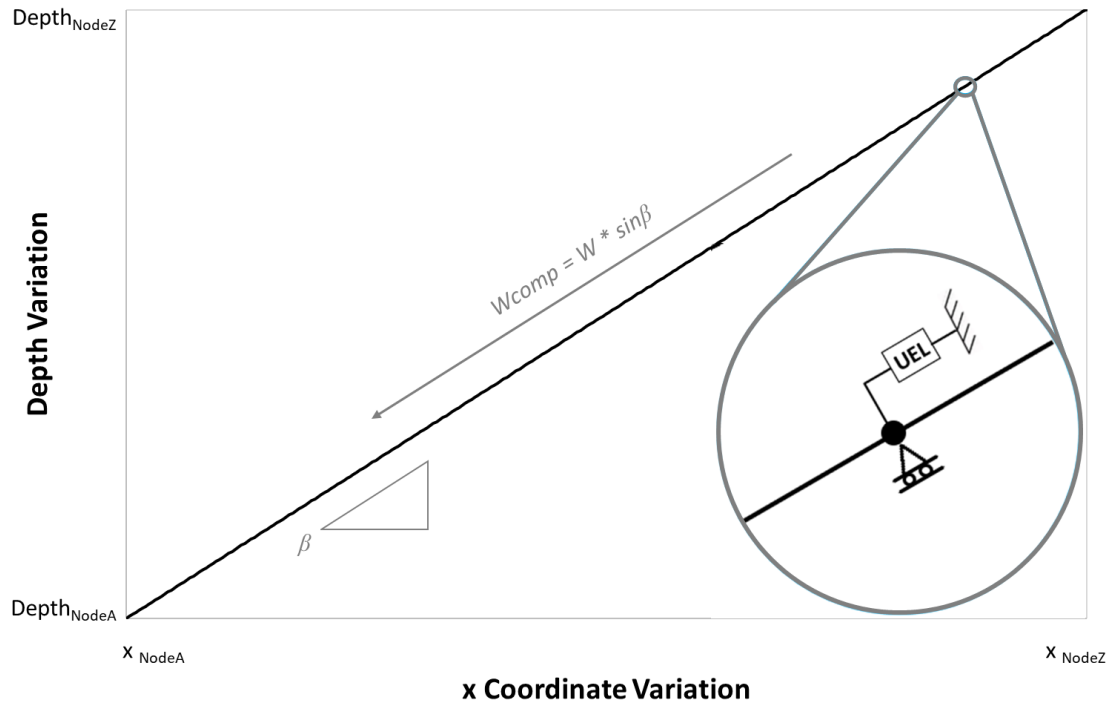


430

431

432

433 **Figure 5 Finite element model sketch**

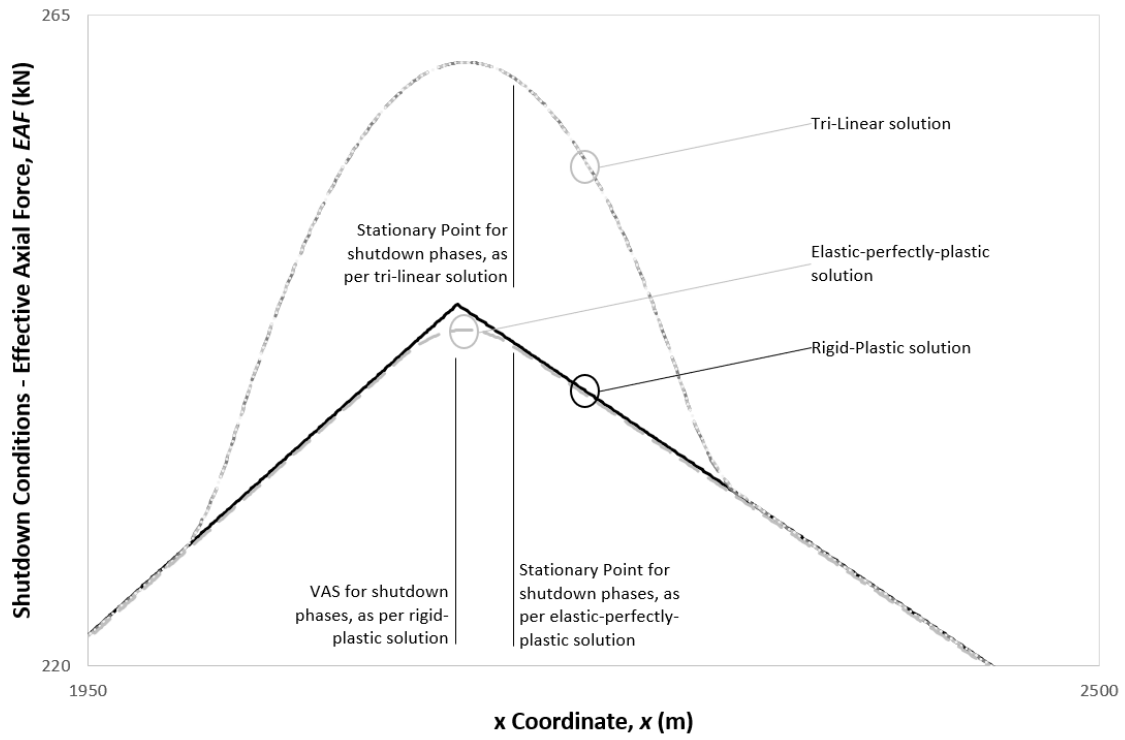


434

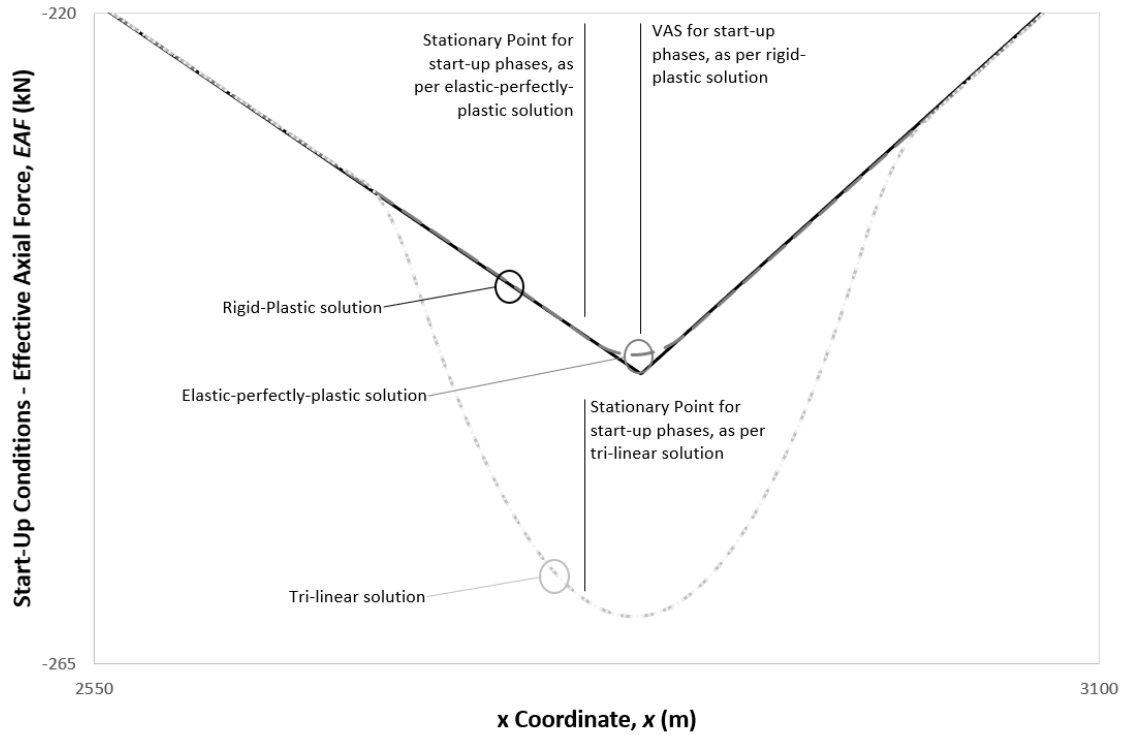
435

436

437 **Figure 6 Effective axial force for tri-linear strategy case ii – EqualPeaks (Zoom)**



438

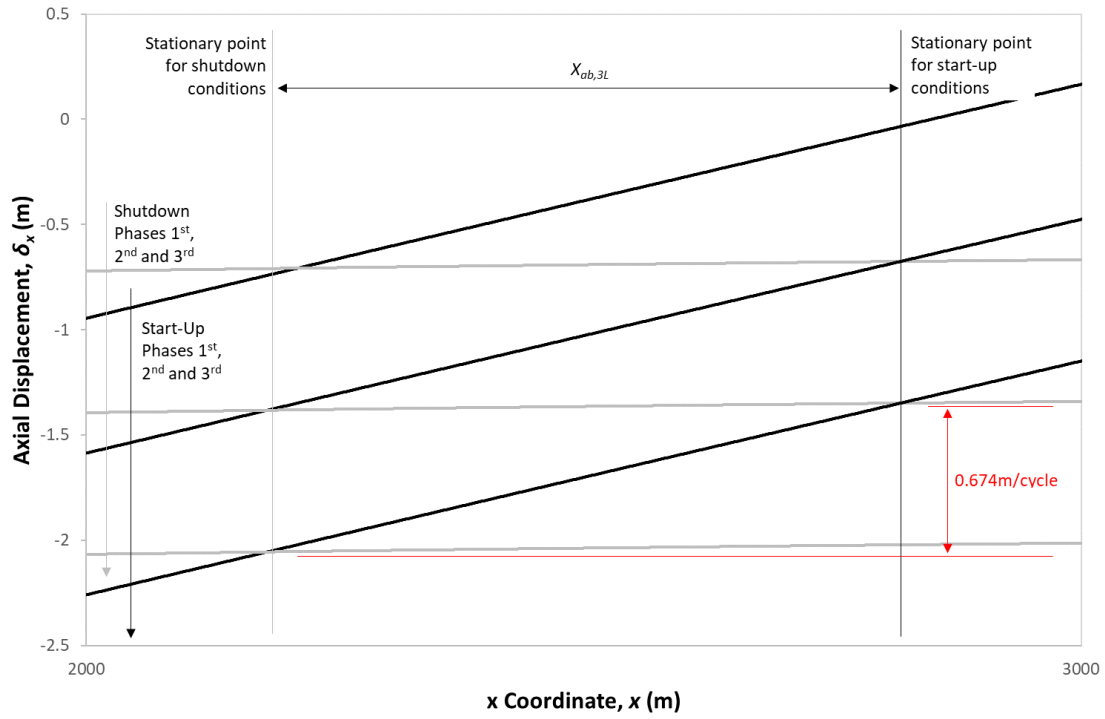


439

440

441

442 **Figure 7 Axial displacement for tri-linear strategy case ii – EqualPeaks (Zoom)**

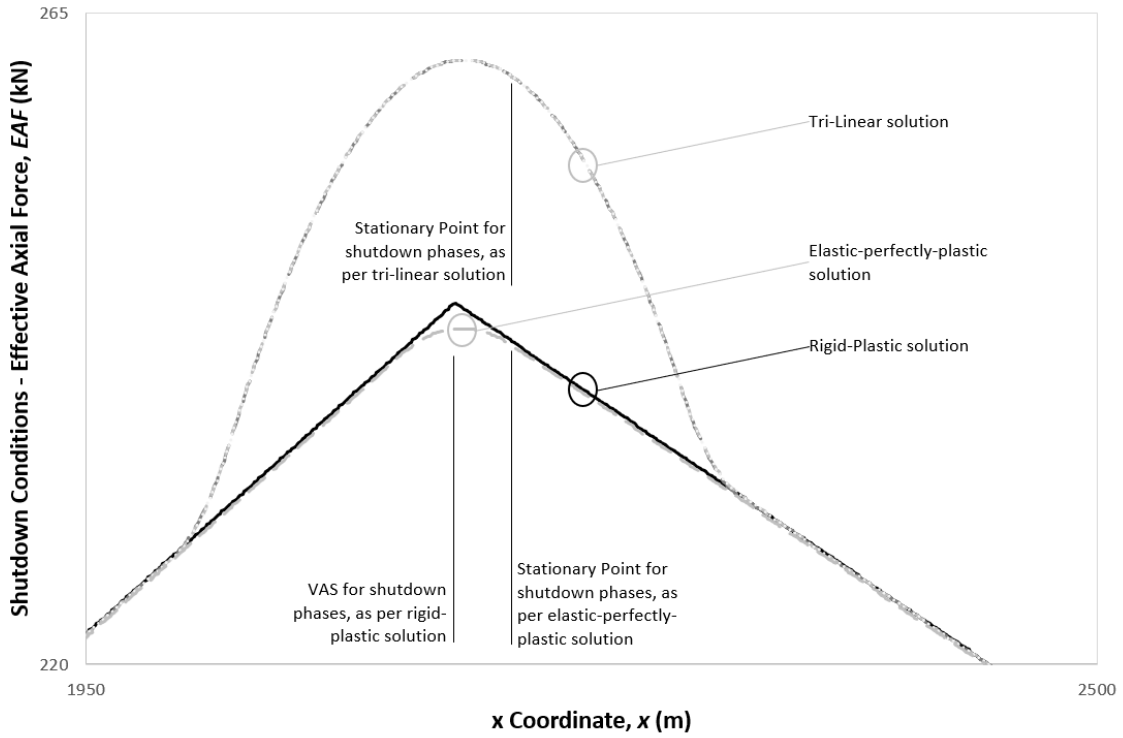


443

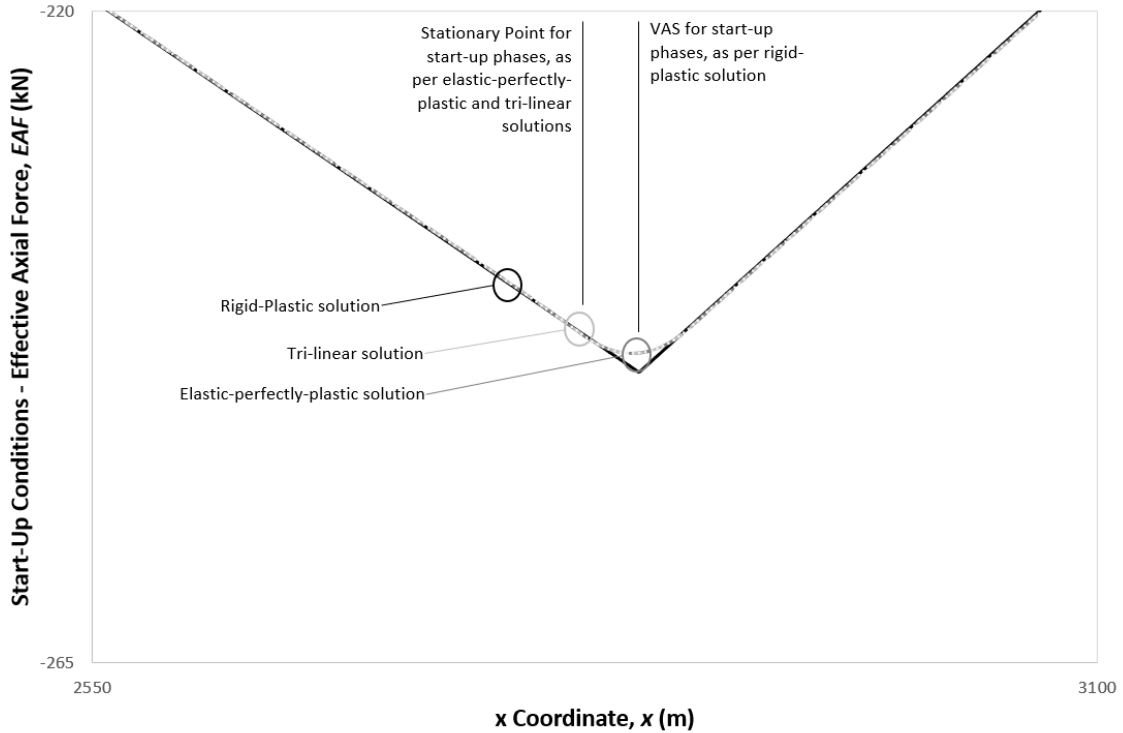
444

445

446 **Figure 8 Effective axial force for tri-linear strategy case ii – NoSupPeak (Zoom)**



447

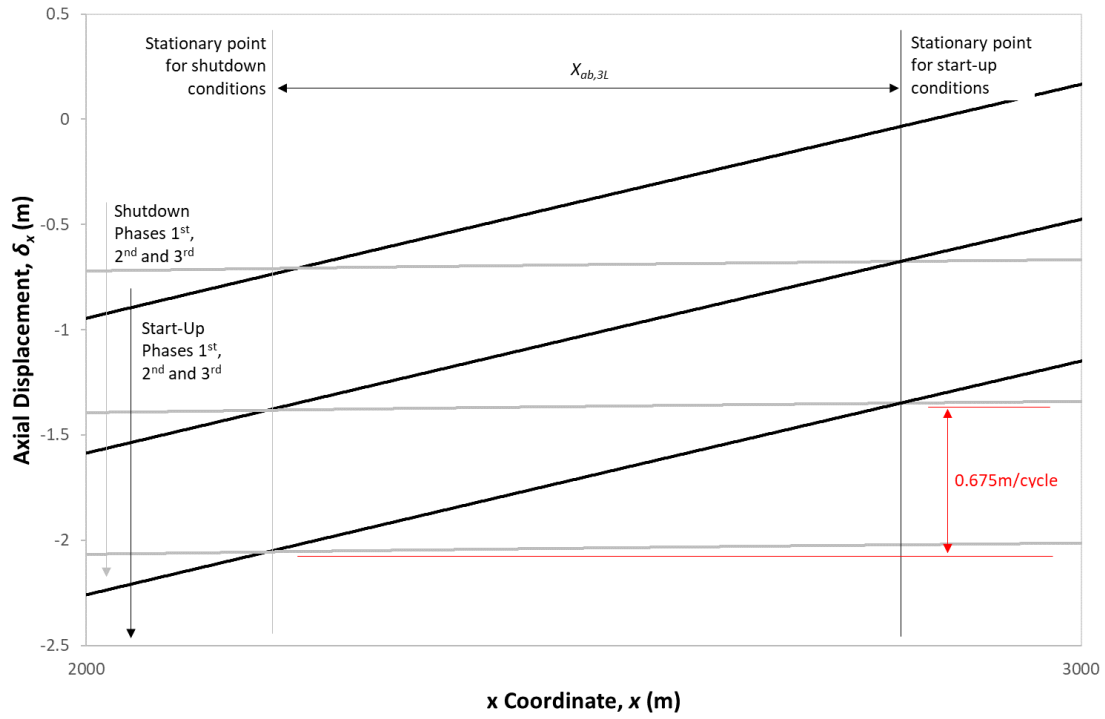


448

449

450

451 **Figure 9 Axial displacement for tri-linear strategy case ii– NoUpPeak (Zoom)**

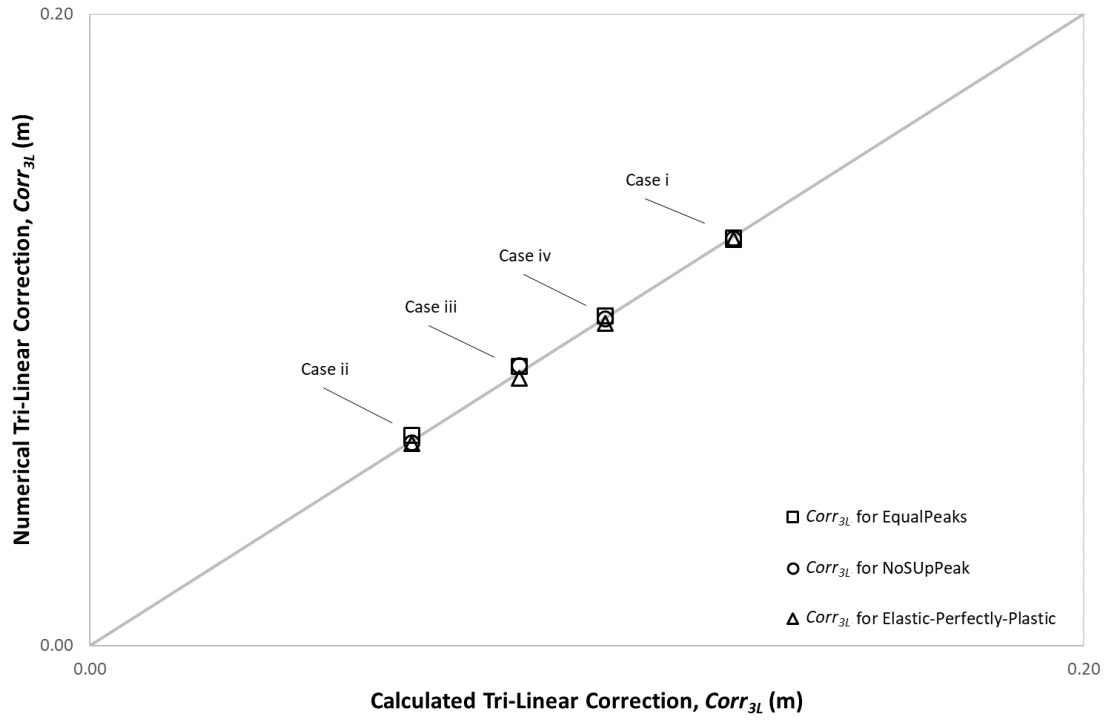


452

453

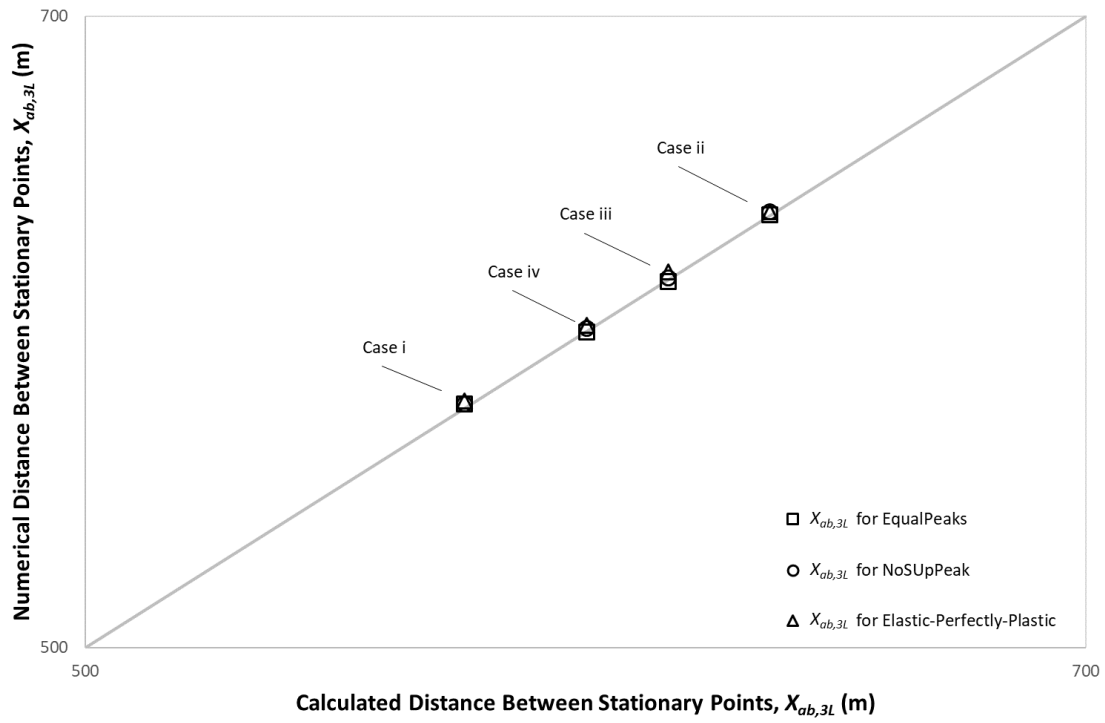
454

455 **Figure 10 Tri-linear correction results**



456
457

458 **Figure 11 Distance between stationary points results**

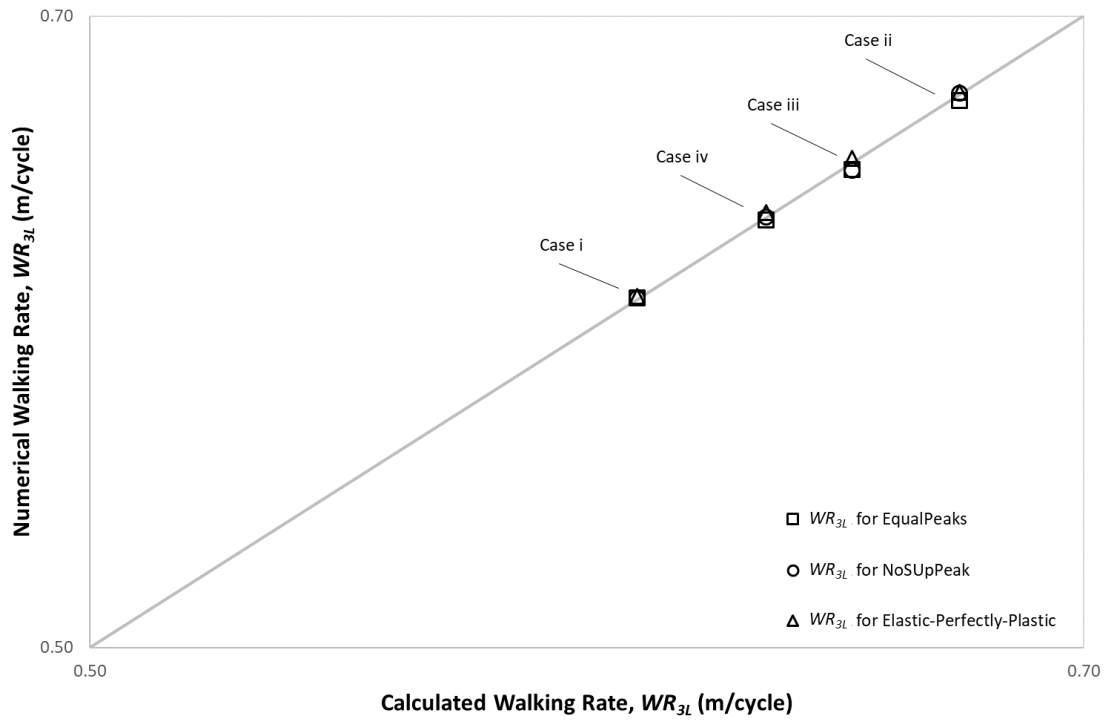


459

460

461

462 **Figure 12** Walking rate results



463
464

465

466 **TABLES**467 **Table 1 General properties**

Parameter	Value
Steel outside diameter, OD	0.3239 m
Steel wall thickness, t	0.0206 m
Length, L	5000 m
Seabed slope angle, θ	2.0 °
Temperature variation, ΔT	100 °C
Pipe submerged weight, W	0.4 kN/m
Residual friction coefficient, μ	0.25
Steel Young's modulus, E	2.07×10^{11} Pa
Steel Poisson coefficient, ν	0.3
Steel thermal expansion coefficient, α	1.165×10^{-5} °C ⁻¹

468

469

470 **Table 2 Case properties**

Property	Cases			
	i	ii	iii	iv
Peak Elastic Force, F_P (kN)	0.200	0.400	0.300	0.250
Peak Elastic Force Mobilisation Displacement, δ_{mobP} (m)	0.129	0.129	0.129	0.129
Residual Plastic Force, F_R (kN)	0.100	0.100	0.100	0.100
Residual Plastic Force Mobilisation Displacement, δ_{mobR} (m)	0.162	0.162	0.162	0.162
Ideal Mobilisation Displacement, $\delta_{mob'}$ (m)	0.065	0.032	0.043	0.052

471

472

473 **Table 3 Tri-linear finite element analysis results for soil case ii**

Case	Distance Between Stationary Points	Walking Rate
ii	EqualPeaks	0.674 m/cycle
	NoSUpPeak	0.675 m/cycle

474

475

476 **Table 4 Rigid-plastic calculation results**

Case	Distance Between Stationary Points	Walking Rate
Rigid-plastic (Carr <i>et al.</i> , 2006)	698 m	0.740 m/cycle

477

478

479 **Table 5 Analytical results**

Case	Distance Between Stationary Points	Walking Rate
i	576 m	0.610 m/cycle
ii	637 m	0.675 m/cycle
iii	617 m	0.653 m/cycle
iv	600 m	0.636 m/cycle

480

481

482 **Table 6 Tri-linear finite element analyses results**

Case		Distance Between Stationary Points	Walking Rate
i	EqualPeaks	577 m	0.611 m/cycle
	NoSUpPeak	577 m	0.611 m/cycle
ii	EqualPeaks	637 m	0.674 m/cycle
	NoSUpPeak	638 m	0.675 m/cycle
iii	EqualPeaks	616 m	0.652 m/cycle
	NoSUpPeak	617 m	0.653 m/cycle
iv	EqualPeaks	600 m	0.635 m/cycle
	NoSUpPeak	601 m	0.636 m/cycle

483